

Time-delayed and stochastic effects in a predator–prey model with ratio dependence and Holling type III functional response

Cite as: Chaos 31, 073141 (2021); doi: 10.1063/5.0055623

Submitted: 30 April 2021 · Accepted: 7 July 2021 ·

Published Online: 29 July 2021



View Online



Export Citation



CrossMark

K. B. Blyuss,^{1,a)}  S. N. Kyrychko,²  and Y. N. Kyrychko¹ 

AFFILIATIONS

¹Department of Mathematics, University of Sussex, Brighton BN1 9QH, United Kingdom

²Poljakov Institute of Geotechnical Mechanics, National Academy of Sciences of Ukraine, Simferopolska Str. 2a, Dnipro 49005, Ukraine

Note: This paper is part of the Focus Issue, In Memory of Vadim S. Anishchenko: Statistical Physics and Nonlinear Dynamics of Complex Systems.

a) Author to whom correspondence should be addressed: k.blyuss@sussex.ac.uk

ABSTRACT

In this article, we derive and analyze a novel predator–prey model with account for maturation delay in predators, ratio dependence, and Holling type III functional response. The analysis of the system's steady states reveals conditions on predation rate, predator growth rate, and maturation time that can result in a prey-only equilibrium or facilitate simultaneous survival of prey and predators in the form of a stable coexistence steady state, or sustain periodic oscillations around this state. Demographic stochasticity in the model is explored by means of deriving a delayed chemical master equation. Using system size expansion, we study the structure of stochastic oscillations around the deterministically stable coexistence state by analyzing the dependence of variance and coherence of stochastic oscillations on system parameters. Numerical simulations of the stochastic model are performed to illustrate stochastic amplification, where individual stochastic realizations can exhibit sustained oscillations in the case, where deterministically the system approaches a stable steady state. These results provide a framework for studying realistic predator–prey systems with Holling type III functional response in the presence of stochasticity, where an important role is played by non-negligible predator maturation delay.

Published under an exclusive license by AIP Publishing. <https://doi.org/10.1063/5.0055623>

Recent years have witnessed an explosion of interest in different aspects of modelling biological interactions, driven both by new ecological evidence and by theoretical advances. One particular class of models that have attracted particular attention are models with ratio dependence, where the per-capita rate of predation depends on the ratio between predator and prey populations. Motivated by recent work on plant diseases based on plant–insect interactions, in which insects are the predators feeding on plants playing the role of food source, we have proposed a new predator–prey model with ratio dependence and a Holling type III (sigmoidal) functional response. Predator population in the model is assumed to be maturing with a non-negligible maturation time, which is explicitly included in the model in the form of time delay. We explore the role of different parameters and time delay and show that the model always supports a prey-only equilibrium, which is stable if the predation rate is

sufficiently small or when the predators take too long to mature. In the opposite case, the model can exhibit coexistence, where both prey and predators are present, and the conditions for biological feasibility and stability of this steady state are established depending on different parameters. The model is also reformulated as a stochastic delayed system to explore the role of demographic stochasticity in the dynamics of predator–prey interactions. We derive equations for stochastic fluctuations around the deterministically stable coexistence steady state and use these to quantify the variance and coherence of these fluctuations. Numerical simulations illustrate how even when the coexistence steady state is deterministically stable, in individual stochastic realizations, the model still exhibits stochastic oscillations around it, which can have major implications for understanding the dynamics of interactions between real biological species.

I. INTRODUCTION

Ever since the pioneering work of Lotka¹ and Volterra,² mathematical models of predator–prey type have provided tremendous insights into the dynamics of interactions between different species or, more widely, between interacting agents that have found application not only in biology but also in a diversity of other areas, from immunology to economics.^{3–6} The starting point for many of these models in ecological context is a general predator–prey model of Gause–Kolmogorov type,^{7–9}

$$\begin{aligned}\dot{u} &= uf(u) - vg(u, v), \\ \dot{v} &= bvg(u, v) - dv,\end{aligned}$$

where $u(t)$ and $v(t)$ are abundances or population densities of prey and predator, respectively; $f(u)$ describes the intrinsic per-capita growth rate of prey in the absence of predator; and d is the predator's natural death rate. In order to guarantee boundedness of prey population, the function $f(u)$ is often chosen in the form of a monotonically decreasing linear function $f(u) = r(1 - u/K)$, which biologically describes an intra-specific prey competition and corresponds to the logistic growth of prey with linear growth rate r and carrying capacity K . Function $g(u, v)$ is known as the *trophic function* or the so-called *functional response* of the predator,¹⁰ and it quantifies how efficiently predators are consuming prey and how this enhances their own reproduction. To account for the details of the process of predators searching for prey and, more specifically, for the idea that at higher predator densities, predators would have to share some of the prey, Arditi and Ginzburg^{11,12} proposed that at the time scales of population dynamics, the overall rate of predation is better represented by a function that depends on the ratio of prey to predators. To this end, they suggested choosing the trophic function $g(u, v)$ in the form $g(u/v)$,

$$\begin{aligned}\dot{u} &= uf(u) - vg\left(\frac{u}{v}\right), \\ \dot{v} &= bvg\left(\frac{u}{v}\right) - dv,\end{aligned}$$

which is known as *ratio dependence*. Subsequently, besides a large number of theoretical models with ratio dependence,^{13–19} several field and experimental studies^{2,20,21} have also provided support for using ratio-dependence predation as a more realistic representation of predator–prey dynamics.

While in the classical Lotka–Volterra model, the trophic function g is simply proportional to the number of prey $g(u) = au$, a more realistic representation that has become one of the most commonly used in ecology was suggested by Holling.^{22,23} It accounts for two distinct aspects of interaction between prey and predators, namely, predators searching for prey and predators handling (i.e., chasing, killing, and digesting) the prey. Holling proposed three types of functional response $g(u)$, which all satisfy $g(0) = 0$, they all approach some constant for large values of u , and the difference is in their behavior for smaller prey numbers/densities. Type I response is linearly increasing for small prey densities, whereas for large prey numbers it saturates at some constant value; type II and type III are also functions that are saturating at high prey numbers and are, respectively, concave and sigmoidal. In this article, we are interested in Holling type III functional response, which is a sigmoidal function

and is often represented in the form,^{24,25}

$$g(z) = \frac{az^n}{1 + ahz^n}, \quad n > 1.$$

A large number of authors have analyzed predator–prey models with this type of functional response and ratio dependence, both without^{26–28} and with time delays,^{29–31} as well as with spatial dependence.^{32–34} Holling type III response with prey dependence and ratio dependence has been observed in a number of experimental settings.^{35–38} In this article, we will instead consider the following form of the Holling type III functional response:

$$g(z) = ae^{-a/z},$$

which satisfies the conditions of $g(0) = 0$, is monotonically increasing, and settles at a constant value as $z \rightarrow \infty$. This functional response is reminiscent of the Ivlev (Holling II) trophic function $g(z) = a(1 - e^{-az})$ ^{39,40} and of the Ricker model⁴¹ for single-species populations. It is also not entirely dissimilar from a logistic-type term of the form $g(u, v) = a(1 - v/u)$ used in models of plant–insect interactions, where plants serve as hosts for insect predators, and current plant population represents carrying capacity for insect population.^{42,43} With account for ratio dependence, we, therefore, have the trophic function $g(u, v)$ in the form,

$$g(u, v) = ae^{-av/u}. \quad (1)$$

A recent work has used a delayed version of this trophic function to analyze the dynamics of vector–plant interactions in the context of modelling plant mosaic disease.⁴⁴

The last aspect we want to include in our model is the idea that predators normally take some time to mature, and only mature predators can reproduce. Mathematically, this is often represented by stage-structured models that separate populations into immature and mature individuals and include a *maturation delay*, which describes the period of time it takes for immature individuals to reach maturity when they start to reproduce.^{45–48} Including maturation delay in the above model, we obtain the following system:

$$\begin{aligned}\dot{u} &= ru\left(1 - \frac{u}{K}\right) - av(t)e^{-av(t)/u(t)}, \\ \dot{v} &= bv(t - \tau)e^{-av(t-\tau)/u(t-\tau)}e^{-d\tau} - dv,\end{aligned} \quad (2)$$

which represents a predator–prey model with ratio dependence and Holling type III function response and which will be studied in this article. Here, a is the predation or consumption rate, b is the conversion rate from prey into predator biomass, τ is the maturation delay, $v(t)$ represents the population of mature predators, and the factor $e^{-d\tau}$ represents the fraction of newly born predators that have survived to maturation. It is easy to show that this model is well-posed in that for any non-negative initial condition, its solutions will remain non-negative and bounded.

Rescaling the variables and parameters,

$$\begin{aligned}u &= K\hat{u}, \quad v = K\hat{v}, \quad dt = \hat{t}, \quad d\tau = \hat{\tau}, \\ \frac{r}{d} &= \hat{r}, \quad \frac{a}{d} = \hat{a}, \quad \frac{b}{d} = \hat{b},\end{aligned}$$

the model (2) can be rewritten as follows:

$$\begin{aligned} \dot{u} &= ru(1 - u) - av(t)e^{-\alpha v(t)/u(t)}, \\ \dot{v} &= bv(t - \tau)e^{-\alpha v(t-\tau)/u(t-\tau)}e^{-\tau} - v, \end{aligned} \tag{3}$$

where we have dropped hats for notational convenience.

The remainder of this article is organized as follows. In Sec. II, we find steady states of model (3), derive conditions for their biological feasibility, and study their stability, both analytically and using numerical computations. To understand the role of intrinsic stochasticity of finite population sizes, in Sec. III, we develop and analyze a stochastic version of the model, with an emphasis on deriving analytical expressions for spectra of fluctuations around the deterministically stable coexistence steady state. This will be used to numerically compute variance and coherence of stochastic oscillations depending on system parameters. In that section, we will also solve the stochastic model numerically and compare its solutions to that of the deterministic model to illustrate the phenomenon of stochastic amplification. The article concludes in Sec. IV with a discussion of results.

II. STEADY STATES AND THEIR STABILITY

For any values of parameters, the model (3) has a prey-only steady state $E_p = (1, 0)$. In the neighborhood of point $(u, v) = (0, 0)$ in the first quadrant, the term $ve^{-\alpha v/u}$ is well-defined and positive, and in the limit, we have

$$0 \leq |ve^{-\alpha v/u}| \leq |v| \xrightarrow{(u,v) \rightarrow (0,0)} 0,$$

which shows that $E_0 = (0, 0)$ is another steady state of the system that exists for any parameter values and biologically represents the extinction of both species.

Besides the above two steady states, the model can also have a coexistence steady state $E^*(u^*, v^*)$, where

$$u^* = \frac{\alpha \bar{b}r - a \ln(\bar{b})}{\alpha \bar{b}r}, \quad v^* = \frac{\ln(\bar{b}) (\alpha \bar{b}r - a \ln(\bar{b}))}{\alpha^2 \bar{b}r}, \tag{4}$$

where $\bar{b} = be^{-\tau}$. In order for this steady state to be biologically feasible, i.e., to have both of its components positive, one has to require $\bar{b} > 1$ (which immediately implies $b > 1$) and

$$\alpha \bar{b}r - a \ln \bar{b} > 0 \iff \frac{\alpha r}{a} - \frac{\ln (be^{-\tau})}{be^{-\tau}} > 0.$$

This last conditions can be written as $h(z) > 0$, where

$$h(z) = c - \frac{\ln (be^{-\tau})}{be^{-\tau}}, \quad c = \frac{\alpha r}{a}.$$

Function $h(z)$ is convex, with two branches going up from a global minimum, which is located at $z_0 = \ln(b) - 1$. Depending on whether z_0 and $h(z_0)$ are positive or negative, the function $h(z)$ can have zero, one, or two real positive roots. This gives the following restrictions on maturation delay τ , for which the coexistence steady

state is biologically feasible:

$$\begin{aligned} 1 < b \leq e : & \begin{cases} c \in (0, \ln(b)/b], & \tau \in [\tau_2, \tau_{\max}], \\ c \in (\ln(b)/b, \infty), & \tau \in [0, \tau_{\max}], \end{cases} \\ b > e : & \begin{cases} c \in (0, \ln(b)/b], & \tau \in [\tau_2, \tau_{\max}], \\ c \in (\ln(b)/b, 1/e], & \tau \in [0, \tau_1] \cup [\tau_2, \tau_{\max}], \\ c \in (1/e, \infty), & \tau \in [0, \tau_{\max}], \end{cases} \end{aligned} \tag{5}$$

where

$$\tau_1 = -\ln\left(-\frac{W_{-1}(c)}{cb}\right), \quad \tau_2 = -\ln\left(-\frac{W_0(c)}{cb}\right), \quad \tau_{\max} = \ln(b),$$

and $W_0(\cdot)$ and $W_{-1}(\cdot)$ are Lambert functions with $k = 0$ (principal branch) and $k = -1$.

The characteristic equation for the linearization of the system (3) near the steady state E_p has the form,

$$(\lambda + r) \cdot (be^{-\tau}e^{-\lambda\tau} - 1 - \lambda) = 0,$$

which shows that one of the eigenvalues is $\lambda = -r < 0$, and other eigenvalues satisfy a transcendental equation

$$\lambda = be^{-\tau}e^{-\lambda\tau} - 1. \tag{6}$$

For $\tau = 0$, the condition for stability, i.e., $\text{Re}(\lambda) < 0$, becomes $\bar{b} < 1$, which simplifies to $b < 1$. Let us assume the condition

$$\bar{b} < 1 \iff be^{-\tau} < 1 \tag{7}$$

also holds for $\tau > 0$. To check, whether or not the steady state E_p is stable, we look for roots of Eq. (6) in the form $\lambda = \rho + i\kappa$. Substituting this into (6) and separating real and imaginary parts yields

$$\begin{aligned} \rho &= \bar{b}e^{-\tau\rho} \cos(\tau\kappa) - 1, \\ \kappa &= \bar{b}e^{-\tau\rho} \sin(\tau\kappa). \end{aligned}$$

Since $\bar{b} < 1$, the first of these equations has no roots with $\rho > 0$, which implies that the steady state E_p is stable. If $\bar{b} > 1$, due to the definition of \bar{b} , this means that $b > 1$, and hence, the steady state E_p is unstable already at $\tau = 0$, though the analysis we have just performed shows that this steady state can get stabilized for sufficiently large τ , provided the condition (7) holds. For a fixed value of $b > 1$, the loss of stability of the steady state E_p occurs at

$$\tau_c = \ln(b), \tag{8}$$

with E_p being stable for $\tau > \tau_c$ and unstable for $\tau < \tau_c$. We note that the condition $\bar{b} > 1$ for instability of E_p is also one of the conditions for biological feasibility of the coexistence steady state E^* . Since parameters in the model (3) have been rescaled using d , whose inverse is the average life expectancy of predators, this suggests an additional biological constraint of $\tau \leq 1$ to avoid a possibility of maturation time exceeding the overall life expectancy. This restriction implies that for $b > e$, the prey-only equilibrium E_p is unstable within the entire range of possible maturation delays $0 \leq \tau \leq 1$.

For the coexistence steady state E^* , the characteristic equation has the following form:

$$\begin{vmatrix} r \left(2 \frac{a \ln(\bar{b})}{\alpha \bar{b} r} - 1 \right) - \frac{a [\ln(\bar{b})]^2}{\alpha \bar{b}} - \lambda & -\frac{a(1 - \ln(\bar{b}))}{\bar{b}} \\ \frac{[\ln(\bar{b})]^2}{\alpha} e^{-\lambda \tau} & (1 - \ln(\bar{b})) e^{-\lambda \tau} - 1 - \lambda \end{vmatrix} = 0. \tag{9}$$

For $\tau = 0$, this simplifies to a quadratic equation

$$\lambda^2 - \lambda \left[-\ln(b) + r \left(2 \frac{a \ln(b)}{\alpha b r} - 1 \right) - \frac{a [\ln(b)]^2}{\alpha b} \right] + \ln(b) \left(r - \frac{a \ln(b)}{\alpha b} \right) = 0,$$

and with the last term being positive to ensure feasibility of the steady state E^* , the condition for stability of E^* at $\tau = 0$ can be readily found as

$$-\ln(b) + r \left(2 \frac{a \ln(b)}{\alpha b r} - 1 \right) - \frac{a [\ln(b)]^2}{\alpha b} < 0.$$

Since the coefficients of the characteristic equation themselves depend on τ through $\bar{b} = b e^{-\tau}$, for $\tau > 0$ it does not prove possible to obtain closed form explicit conditions for stability of the steady state E^* . Hence, we compute characteristic eigenvalues numerically using traceDDE.⁵²

For the extinction steady state E_0 , we note that the system (3) is not differentiable at this steady state; hence, the stability analysis of this steady state cannot be performed in a standard fashion. A standard approach to the analysis of stability of extinction steady state in systems with ratio dependence is the so-called Briot-Bouquet transformation that replaces the variable v by a new variable z defined as $v = zu$.⁴⁹⁻⁵¹ In the particular case of system (3), due to the fact

that the ratio-dependent term is instantaneous in one equation and time-delayed in another equation, such a transformation would not remove the singularity in the Jacobian at the point (0, 0). However, since solutions to the system (3) are always non-negative and bounded, and the axes $u = 0$ and $v = 0$ are invariant manifolds of the system, one can use Poincaré-Bendixson theorem for time-delayed systems^{53,54} to conclude that in the parameter region, where the prey-only equilibrium E_p is unstable, and the coexistence steady state E^* is infeasible, the system approaches a stable extinction steady state E_0 .

Figure 1 shows the bifurcation diagram of the system (3) depending on parameters a , b , and the maturation delay τ . In plot 1(a), we observe that since $b < e$, there is a critical value of maturation delay τ_c , as determined by Eq. (8), such that the prey-only equilibrium E_p is stable for $\tau > \tau_c$ (region D) and unstable for $\tau < \tau_c$, and at $\tau = \tau_c$, it loses stability through steady-state bifurcation. For $\tau < \tau_c$, which biologically means that predators are maturing quite fast, and the sufficiently small predation rate a , we have a stable coexistence equilibrium E^* (region C), where both prey and predator populations are maintained at some steady levels given by Eq. (4). For higher values of a , as the maturation delay τ is decreased, the steady state E^* loses its stability through a supercritical Hopf bifurcation, resulting in the appearance of periodic solutions (region B). For even smaller values of time delay (or higher values of a), once the feasibility boundary of the coexistence steady state is crossed, which is also stability boundary for this steady state, the system approaches a stable extinction steady state E_0 (region A). Numerical solutions to the system (2) in each of these parameter regions are illustrated in Fig. 2.

Similar behavior is observed in Fig. 1(b), where due to the fact that now $b > e$, the prey-only equilibrium E_p is unstable in the entire admissible range of τ values. For smaller values of predation rate a and small maturation time τ , we have a stable coexistence steady state E^* . If the predation rate is sufficiently small, the coexistence steady state remains stable in the entire range of τ values. However,

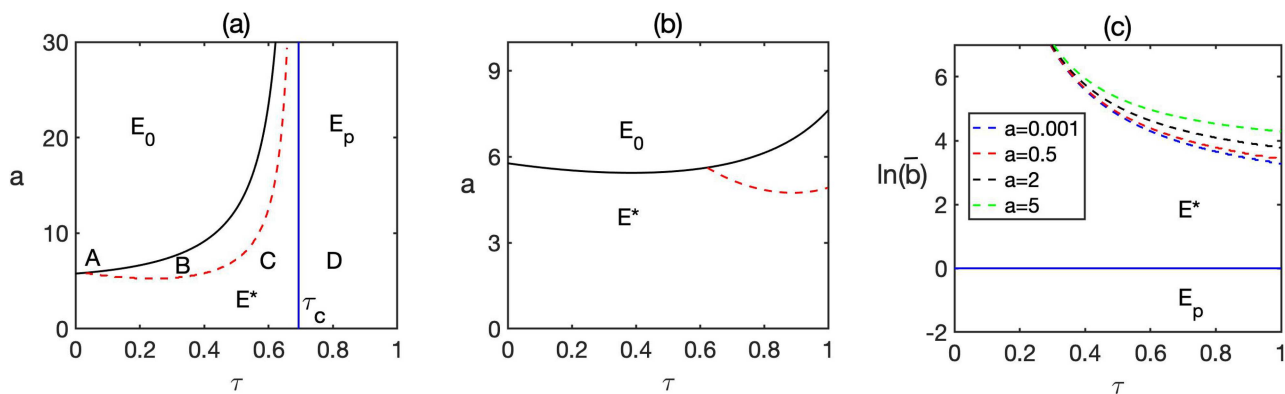


FIG. 1. Bifurcation diagram of the system (3) in the parameter planes of τ - a (a) and (b) and τ - $\ln(\bar{b})$ (c). Solid blue line denotes stability boundary of the prey-only equilibrium E_p , which is stable for $\tau > \tau_c$ and unstable for $\tau < \tau_c$. Solid black line delineates boundary of feasibility of the coexistence steady state E^* , which is not feasible above this line. Dashed lines indicate the boundary of Hopf bifurcation of the coexistence steady state E^* , with this steady state being stable below the corresponding line, and unstable above the line. In plot (a), A, B, C, and D denote parameter regions of a stable extinction steady state E_0 , periodic solution around the coexistence steady state E^* , stable coexistence steady state E^* , and stable prey-only equilibrium E_p . Parameter values are $r = 2$, $\alpha = 1$. (a) $b = 2$; (b) $b = 4$.

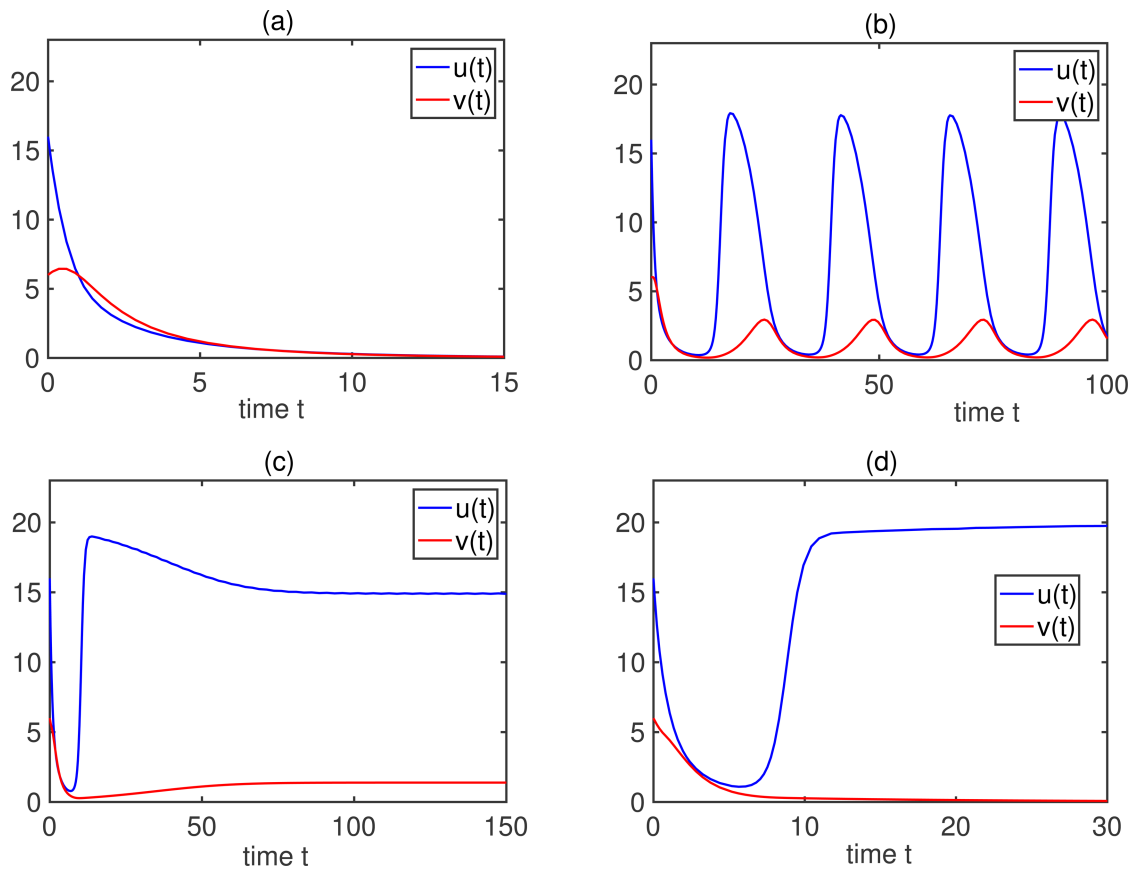


FIG. 2. Numerical solutions to the system (2) in parameter regions A, B, C, and D of Fig. 1(a). Parameter values are $r = 2$, $K = 20$, $\alpha = d = 1$, $b = 2$, $a = 6$, and $(u_0, v_0) = (16, 6)$. (a) $\tau = 0.05$, (b), $\tau = 0.3$, (c) $\tau = 0.6$, and (d) $\tau = 0.8$.

starting with some value of a , as the maturation time increases, this again results in the loss of stability of E^* through a supercritical Hopf bifurcation. In this case, the boundary of feasibility of the steady state E^* at $\tau = \tau_c$ is outside the admissible range of $0 \leq \tau \leq 1$; once the periodic solution emerges, it remains present for all values of τ up to $\tau = 1$. Increasing the predation rate eventually makes the coexistence steady state biologically infeasible (and unstable), which signifies that the rate of predation is so high that the prey is not replenished fast enough to be maintained at some steady level, which, in turn, also drives the predator population down, and the system approaches a stable extinction steady state E_0 .

We also note that as b is reduced to 1, the stability boundary $\tau = \tau_c$ of the steady state E_p comes closer to zero, and for $b < 1$, this steady state is stable for all values of τ , which biologically corresponds to a case, where predator fecundity is too small to maintain predator population, regardless of how quickly it matures. As a result, the coexistence steady state does not exist, and the system always approaches the prey-only equilibrium E_p .

Maturation delay τ plays a dual role in the dynamics of the system (3)—it reduces the fecundity of predators by means of replacing b with \bar{b} , and it also enters the model through delayed values of prey

and predator populations in the predator growth term. To explore separate roles of these two effects, in Fig. 1(c), we plot the bifurcation diagram of the model in terms of maturation delay τ and rescaled predator fecundity \bar{b} . As discussed above, the prey-only steady state E_p loses stability once the value of \bar{b} exceeds $\bar{b} = 1$, at which point the coexistence steady state E^* becomes biologically feasible. For lower values of \bar{b} , the steady state E^* is stable for all admissible values of maturation delay. In contrast, for much higher values of \bar{b} , increasing maturation delay τ results in a destabilization of E^* through a supercritical Hopf bifurcation and the emergence of a stable periodic solution around this steady state. Biologically, this could be interpreted as high fecundity of predators, which results in the higher number of new adult predators, is counterbalanced by the longer time it actually takes for those predators to reach maturity, and it is the balance of those two factors that determines whether the system will exhibit a stable coexistence steady state, observed for smaller \bar{b} and τ , or a periodic solution around this steady state for higher \bar{b} and τ . We also note that increasing the predation rate a has the effect of increasing the size of the parameter region, where the coexistence steady state is stable, with instability occurring at higher values of

\bar{b} and τ . This can be attributed to the fact that increasing a results in a decreased growth of prey population, which means that for the same values of other parameters, lower prey availability facilitates the maintenance of stable coexistence, as is observed in Figs. 1(a) and 1(b).

III. STOCHASTIC MODEL

In order to explore the role of stochasticity in the dynamics, we begin by constructing a continuous-time Markov chain corresponding to the deterministic system (2). To this end, we introduce $X_u, X_v \in \{0, 1, 2, \dots\}$ as discrete random variables representing, respectively, the numbers of prey and predators, with the initial condition $\mathbf{X}(s) = \phi(\mathbf{s}), s \in [-\tau, 0]$. Interpreting prey and predator populations as chemical reactants, we can derive a *delayed chemical master equation* (DCME)^{55,56} corresponding to system (2), in which we separately account for non-delayed reactions, where there is a single time point, where the update happens for both reactants and the products terms, and the *consuming delay* terms, where there are two update points: original reactants are updated at the start of reaction, while the products are updated at the end of the reaction.^{56–58} In the particular case of system (2), the logistic growth term of prey and natural death of predators are non-delayed reactions, whereas predation is a delayed reaction.

If we denote by $P(\mathbf{n}, t)$ the probability of finding the system in the state $\mathbf{n} = (n_u, n_v), n_u, n_v \in \{0, 1, 2, \dots\}$ at time t , i.e., we have

$$P(\mathbf{n}, t) = \text{Prob}[(X_u(t), X_v(t)) = (n_u, n_v) | \phi(\mathbf{s})],$$

then it satisfies the following DCME:

$$\begin{aligned} \frac{\partial P(\mathbf{n}, t)}{\partial t} & b \sum_{\mathbf{m} \in I(\mathbf{n})} m_v(t - \tau) e^{-\alpha m_v(t - \tau)/m_u(t - \tau)} (\varepsilon_v^- - 1) P(\mathbf{n}, t; \mathbf{m}, t - \tau) \\ & + \left\{ r (\varepsilon_u^- - 1) n_u + d (\varepsilon_v^+ - 1) n_v \right. \\ & \left. + a (\varepsilon_u^+ - 1) n_v e^{-\alpha n_v/n_u} + \Omega \frac{r}{N} (\varepsilon_u^+ - 1) \left(\frac{n_u}{\Omega} \right)^2 \right\} P(\mathbf{n}, t), \end{aligned} \tag{10}$$

where $I(\mathbf{n})$ is the set of all possible past states of the system, from which the state \mathbf{n} can be reached via a chain of transitions, $P(\mathbf{n}, t; \mathbf{m}, t - \tau)$ is the joint probability of finding the system in state \mathbf{n} at time t and in state \mathbf{m} at time $t - \tau$, and the shift operators $\varepsilon_{u,v}^\pm$ are defined as follows:

$$\varepsilon_u^\pm f(n_u, n_v) = f(n_u \pm 1, n_v), \quad \varepsilon_v^\pm f(n_u, n_v) = f(n_u, n_v \pm 1).$$

To make further progress in the analysis and, in particular, to get a handle on stochastic fluctuations around the deterministically stable steady state, we perform the system size expansion of the DCME,⁵⁹ which will allow us to separate deterministic and stochastic components. To apply system size expansion to Eq. (10), we anticipate n_u and n_v to be of order Ω , with fluctuations of order $\Omega^{1/2}$,

$$n_u(t) = \Omega u(t) + \Omega^{1/2} \xi_1(t), \quad n_v(t) = \Omega v(t) + \Omega^{1/2} \xi_2(t), \tag{11}$$

where $[u(t), v(t)]$ are determined by the original deterministic model (2) and $[\xi_1(t), \xi_2(t)]$ describe random fluctuations around the deterministic solution. Similarly, we can express delayed variables,⁶⁰

$$\begin{aligned} m_u(t - \tau) &= \Omega u(t - \tau) + \Omega^{1/2} \eta_1(t), \\ m_v(t - \tau) &= \Omega v(t - \tau) + \Omega^{1/2} \eta_2(t). \end{aligned} \tag{12}$$

One can then express probability distributions $P(\mathbf{n}, t)$ and $P(\mathbf{n}, t; \mathbf{m}, t - \tau)$ in terms of $\boldsymbol{\xi} = (\xi_1, \xi_2)^T$ and $\boldsymbol{\eta} = (\eta_1, \eta_2)^T$ as

$$\begin{aligned} P(\mathbf{n}, t) &= P(\Omega(u, v))^T + \Omega^{1/2} \boldsymbol{\xi}^T, t) = \Pi(\boldsymbol{\xi}, t), \\ P(\mathbf{n}, t; \mathbf{m}, t - \tau) &= \Pi(\boldsymbol{\xi}, t; \boldsymbol{\eta}, t - \tau), \end{aligned}$$

which then implies

$$\frac{\partial P(\mathbf{n}, t)}{\partial t} = \frac{\partial \Pi}{\partial t} - \Omega^{1/2} \dot{u} \frac{\partial \Pi}{\partial \xi_1} - \Omega^{1/2} \dot{v} \frac{\partial \Pi}{\partial \xi_2}. \tag{13}$$

Expanding this equation in powers of Ω , at the order $\Omega^{1/2}$, one recovers the system (2) describing deterministic dynamics, and at the next order, i.e., at order Ω^0 , one obtains a delayed Fokker–Planck equation that describes stochastic oscillations around the deterministic trajectory (see the Appendix). Following the methodology of Galla⁶⁰ (see also^{61–64}), we can use this delayed Fokker–Planck equation to obtain the following system of Langevin equations describing the dynamics of fluctuations around a deterministic steady state (u^*, v^*) of the model (2):

$$\begin{aligned} \dot{\xi}_1 &= r \left(1 - \frac{2u^*}{K} \right) \xi_1 - \frac{ad}{b} [(1 - F) \xi_2 + F^2 \xi_1] + \zeta_1, \\ \dot{\xi}_2 &= d [(1 - F) \xi_2(t - \tau) + F^2 \xi_1(t - \tau) - \xi_2(t)] + \zeta_2, \end{aligned} \tag{14}$$

where

$$F = \frac{\ln(\bar{b}/d)}{\alpha}$$

and $\boldsymbol{\zeta}(t) = (\zeta_1(t), \zeta_2(t))^T$ is a vector of two independent Gaussian white noise variables with zero mean, and the noise correlators are given by

$$\begin{aligned} \langle \zeta_1(t) \zeta_1(t') \rangle &= 2ru^* \delta(t - t'), \quad \langle \zeta_2(t) \zeta_2(t') \rangle = 2dv^* \delta(t - t'), \\ \langle \zeta_1(t) \zeta_2(t') \rangle &= 0. \end{aligned}$$

The deterministic part of these equations is exactly the same as what can be obtained directly from system (2) after linearizing it near a steady state (u^*, v^*) , while the noise covariance matrix describing large-scale oscillations around this steady state can only be derived from the system size expansion of the DCME.^{68,69} The Fourier transform of system (14) can be found as

$$M(\omega) \tilde{\boldsymbol{\xi}}(\omega) = \tilde{\boldsymbol{\zeta}}(\omega),$$

where

$$M = \begin{pmatrix} i\omega - r \left(1 - \frac{2u^*}{K} \right) + \frac{adF^2}{b} & \frac{ad}{b} (1 - F) \\ -dF^2 e^{-i\omega\tau} & i\omega + d [1 - (1 - F)e^{-i\omega\tau}] \end{pmatrix}.$$

Introducing the matrix of spectra $S(\omega)$ as $S_{ij}(\omega) = \langle \tilde{\xi}_i(\omega)\tilde{\xi}_j(\omega') \rangle$, we then have

$$S(\omega) = M(\omega)^{-1} \langle \tilde{\zeta}(\omega)\tilde{\zeta}(\omega')^\dagger \rangle (M(\omega)^\dagger)^{-1}, \tag{15}$$

where \dagger denotes Hermitian conjugate, and

$$\langle \tilde{\zeta}(\omega)\tilde{\zeta}(\omega')^\dagger \rangle = \begin{pmatrix} 2ru^* & 0 \\ 0 & 2dv^* \end{pmatrix} \delta(\omega + \omega').$$

This then gives the power spectra of fluctuations in prey and predators around the coexistence steady state as

$$P_u(\omega) = \langle |\xi_1|^2 \rangle = \frac{2 \left(ru^* |i\omega + d - d(1-F)e^{-i\omega\tau}|^2 + dv^* \left[\frac{ad}{b}(1-F) \right]^2 \right)}{|\det(M)|^2},$$

$$P_v(\omega) = \langle |\xi_2|^2 \rangle = \frac{2 \left(ru^* d^2 F^4 + dv^* \left[\left(r \left(1 - \frac{2u^*}{K} \right) - \frac{adF^2}{b} \right)^2 + \omega^2 \right] \right)}{|\det(M)|^2}, \tag{16}$$

with

$$|\det(M)|^2 = \left[\omega d \left(1 + \frac{adF^2}{b} - (1-F) \cos \omega\tau \right) - r \left(1 - \frac{2u^*}{K} \right) (\omega + (1-F) \sin \omega\tau) \right]^2 + \left[rd \left(1 - \frac{2u^*}{K} \right) ((1-F) \cos \omega\tau - 1) - \omega(\omega + d(1-F) \sin \omega\tau) + \frac{adF^2}{b} \right]^2.$$

The power spectrum of fluctuations in prey population is shown in Fig. 3. One can observe that increasing the predation rate a makes the dominant frequency of oscillations more pronounced, while

increasing the maturation delay makes the dominant frequency smaller, though this effect is less pronounced for higher values of a , where the system is closer to stability boundary of the coexistence steady state.

When looking at the dynamics of fluctuations around a steady state, the covariance matrix Ξ defined as $\Xi_{ij} = \langle \xi_i(t)\xi_j(t) \rangle - \langle \xi_i(t) \rangle \langle \xi_j(t) \rangle$ is time-independent, and it can be found from the matrix of spectra S as follows:⁶⁵

$$\Xi = \frac{1}{2\pi} \int_{-\infty}^{\infty} S(\omega) d\omega,$$

while for stochastic systems without time delay, one could use a Lyapunov equation to obtain the covariance matrix.^{61,66,67}

The level of fluctuations around the dominant spectral frequency for each of the two populations $X_u(t)$ and $X_v(t)$ around their steady-state values X_u^* and X_v^* can be quantified using their respective mean-square variances

$$A_{u,v} = \lim_{T \rightarrow \infty} \int_{-T}^T [X_{u,v}(t) - X_{u,v}^*]^2 dt = \int_0^\infty 2P_{u,v}(\omega) d\omega.$$

Focusing on particular frequency interval $[\omega_1, \omega_2]$ around the peak frequency in the distribution of $P_{u,v}(\omega)$, one can then compute the quantity

$$A_{u,v}^p = \int_{\omega_1}^{\omega_2} 2P_{u,v}(\omega) d\omega$$

and use this quantity to define the *coherence of stochastic fluctuations* as $c_{u,v} = A_{u,v}^p / A_{u,v}$.^{61,62,68}

Introducing $\mathbf{Y}(t) = (Y_1(t), Y_2(t))^T$ as a vector of two continuous random variables, we can derive the following Itô stochastic delay differential equation model:

$$d\mathbf{Y} = \boldsymbol{\mu} dt + Q d\mathbf{W}(t), \quad \mathbf{Y}(s) = \boldsymbol{\phi}(s), \quad s \in [-\tau, \mathbf{0}], \tag{17}$$

where the drift vector $\boldsymbol{\mu}$ and the matrix Q are given by

$$\boldsymbol{\mu} = \begin{pmatrix} P_1 - P_2 \\ P_3 - P_4 \end{pmatrix}, \quad Q = \begin{pmatrix} \sqrt{P_1 + P_2} & 0 \\ 0 & \sqrt{P_3 + P_4} \end{pmatrix},$$

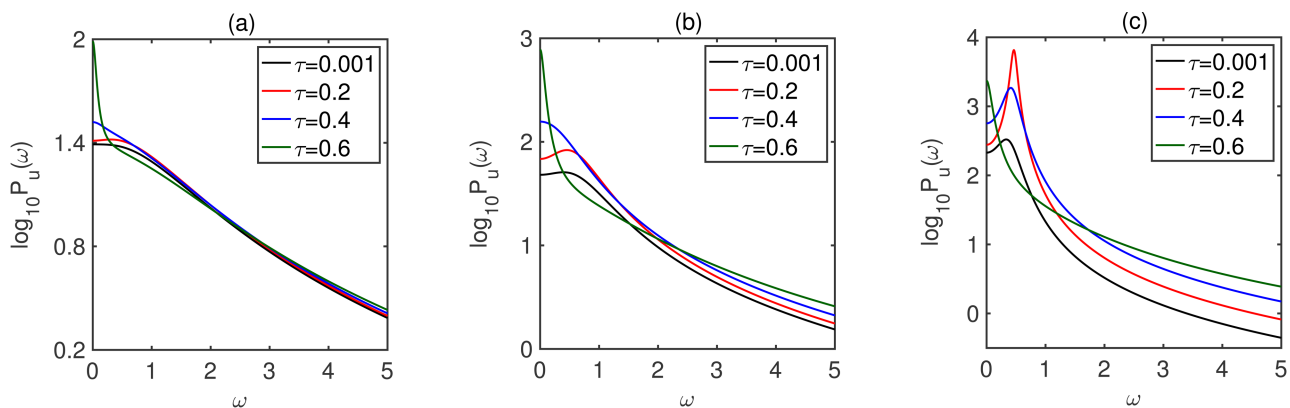


FIG. 3. Power spectra $P_u(\omega)$ of stochastic fluctuations in prey population around the coexistence steady state E^* as given by Eq. (16). Parameter values are $r = 2$, $K = 20$, $\alpha = d = 1$, and $b = 2$. (a) $a = 1$, (b) $a = 3$, and (c) $a = 5$.

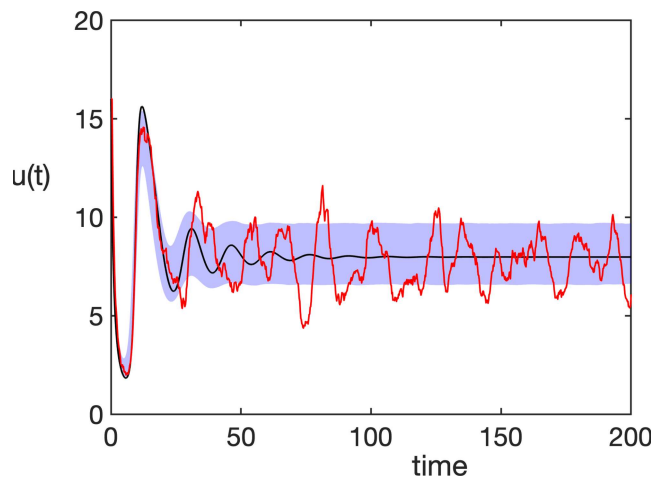


FIG. 4. Numerical solution (black) to the deterministic model (2) shown together with a single stochastic trajectory (red) from (17). Shaded area indicates a region of one standard deviation obtained from the mean of 20 000 simulations. Parameter values are $r = 2$, $K = 20$, $\alpha = d = 1$, $a = 5.5$, and $\tau = 0.4$.

where

$$P_1 = rY_1(t), \quad P_2 = \frac{rY_1(t)^2}{K} + aY_2(t)e^{-\alpha Y_2(t)/Y_1(t)},$$

$$P_3 = \bar{b}Y_2(t - \tau)e^{-\alpha Y_2(t-\tau)/Y_1(t-\tau)}, \quad P_4 = dY_2(t),$$

and $\mathbf{W}(t) = [W_1(t), W_2(t)]^T$ is a vector of two independent Wiener processes. Equation (17) was solved using the strong predictor–corrector method with the implicitness in the drift coefficient being chosen to be equal to 1/7, which ensures the method has the largest stability region.

Figure 4 illustrates the result of a comparison between 20 000 of stochastic realizations obtained by solving the SDDE (17). For chosen parameter values, the coexistence steady state is deterministically stable, with the largest eigenvalues being a pair of complex conjugate eigenvalues with a negative real part. As a result of this, the deterministic trajectory, which coincides with the average of those stochastic simulations, shows the behavior of decaying oscillations toward a stable steady state E^* . In contrast, an individual stochastic realization can still exhibit stochastic oscillations around this deterministically stable steady state. This phenomenon is known as endogenous “stochastic resonance” or *stochastic amplification*^{68–70} of demographic stochasticity. The fundamental point is that sustained oscillations around the deterministically stable steady state are driven not by external noise but rather by intrinsic finite size effects. The ecological importance of this result lies in the observation that even in the absence of other external drivers, such as seasonality or environmental variability, the system can exhibit sustained stochastic oscillations. We also note that similar to the deterministic case, predator population in the stochastic simulation also lags behind the prey population.

In Fig. 5, we explore how the variance and coherence of stochastic fluctuations in prey population around the coexistence steady state change with parameters. For $b < e$, there appears to be little variation in the level of variance of stochastic fluctuations with the value of maturation delay, while increasing predation rate is associated with higher variance. In contrast, for $b > e$, we observe a split of the stable parameter region of the coexistence steady state in two parts: for smaller values of maturation, delay variance is decreasing with a , while for higher values of maturation, it increases with a , particularly in the neighborhood of stability boundary. In terms of coherence, we observe the split of stability region of coexistence steady state into two parts. The first part is represented by the right region in plot (a) or left region in plot (b), where the largest eigenvalue of linearization around E^* is real and negative; hence, deterministically, there are now decaying oscillations around the steady state E^* , and we observe that there is very little difference in the coherence of stochastic oscillations with maturation delay, though it does slowly grow with a . The second part of the stability region of E^* , which corresponds to the left region in plot (a) or right region in plot (b), is characterized by steady state E^* being stable but with the leading eigenvalues being complex. In this case, the system deterministically exhibits decaying oscillations toward this steady state, and there are significantly larger values of coherence, which also demonstrate larger variation with time delay. As the values of a are increased, and we approach the deterministic boundary of Hopf bifurcation of E^* , coherence increases and reaches the value of 1 at the boundary, where stable deterministic oscillations around E^* emerge. When plotted in the τ – \bar{b} parameter plane, the part of the stability region of E^* , where stability eigenvalues for this steady state are complex, is confined to intermediate value of \bar{b} and larger values of τ . In this part of the parameter plane, one observes the lowest values of variance and coherence of stochastic oscillations around the deterministically stable steady state. Similar to what was discussed above, approaching the boundary of Hopf bifurcation, the coherence of stochastic oscillations increases.

IV. DISCUSSION

In this article, we have proposed and analysed a predator–prey model with ratio dependence, Holling type III functional response of Ricker type, and maturation time delay in predators. The model always admits a prey-only equilibrium, and depending on the values of system parameters, it can also have a coexistence steady state with positive values of prey and predator populations. If the predator growth rate is rather small, and the predation rate is large, then there is some minimum maturation delay, for which the coexistence steady state is feasible, while for small predation rates, it is always feasible. In contrast, for higher rates of predator growth and intermediate values of predation, the coexistence steady state is only feasible for small and for large values of maturation delay, and we have identified these critical values of time delays required for feasibility in terms of Lambert W function. Stability conditions have been derived for both steady states, and they show that the coexistence steady state is only feasible when the prey-only equilibrium is unstable. The coexistence steady state can undergo supercritical Hopf bifurcation, giving rise to stable periodic solutions, and numerical simulations have been performed both to identify stability regions

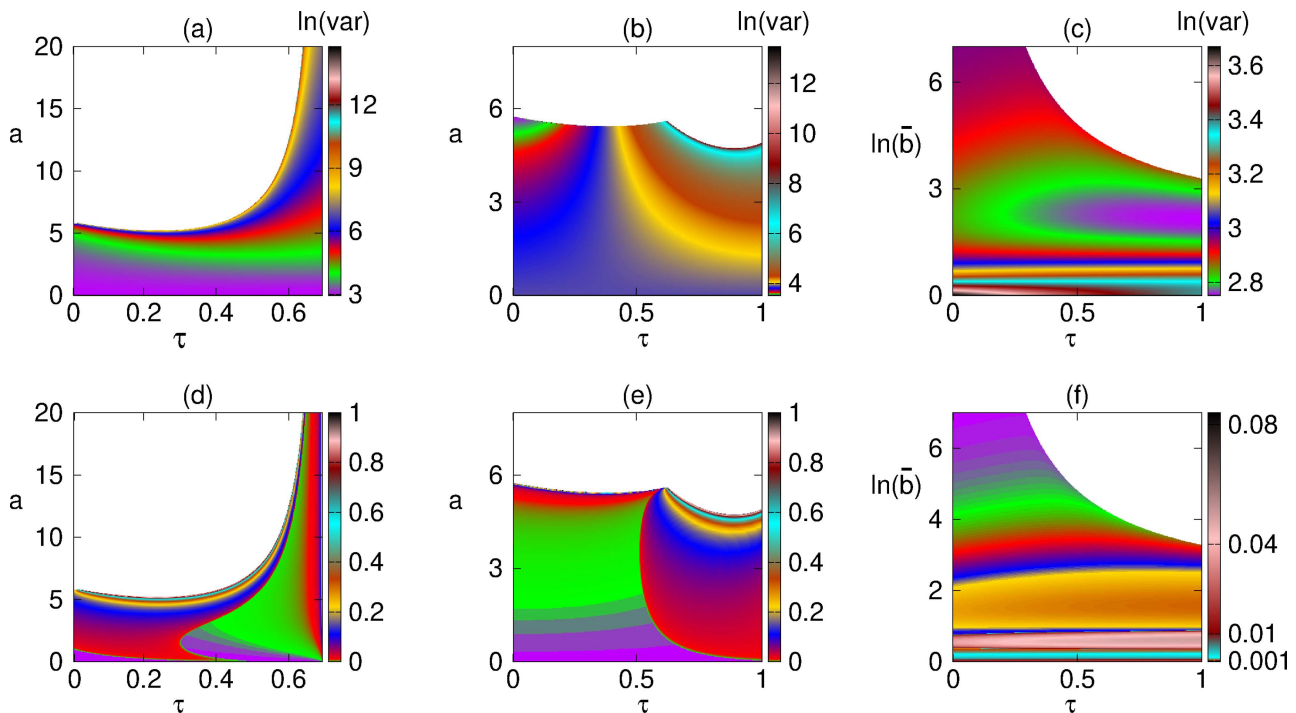


FIG. 5. Variance $\Xi_{u,u}$ (top line) and coherence c_u (bottom line) of stochastic fluctuations in prey population around the coexistence steady state E^* . In the gray region, the steady state E^* is infeasible, and the prey-only steady state E_0 is stable. Parameter values are $r = 2$, $K = 20$, and $\alpha = d = 1$. (a) and (d) $b = 2$; (b) and (e) $b = 4$; (c) and (f) $a = 2$.

of the coexistence steady state and to illustrate the dynamics of the model around it.

To explore the role of demographic stochasticity, we have derived a stochastic counterpart of the model and then applied van Kampen system size expansion to the delayed chemical master equation to obtain a system of equations describing stochastic fluctuations around the deterministically stable coexistence steady state. Due to the linearity of these Langevin equations, it proved possible to obtain spectra of stochastic oscillations in a closed form, and these were then used to study the dependence of variance and coherence of fluctuations on system parameters and maturation delay. The comparison of numerical solution to the Itô SDDE model with the deterministic analog illustrates that while in the limit of very large system size, the system may approach a coexistence steady state that is deterministically stable, individual stochastic realizations still exhibit stochastic oscillations around this state. This result can be important in the context of applying models of this kind to analyze data emerging from ecological observations of real predator–prey interactions.

ACKNOWLEDGMENTS

The authors are grateful to Farzad Fatehi for useful advice regarding numerical simulations of the stochastic model.

APPENDIX: SYSTEM SIZE EXPANSION OF THE MASTER EQUATION

Before proceeding with system size expansion, we rewrite the DCME (10) in the form

$$\begin{aligned} \frac{\partial P(\mathbf{n}, t)}{\partial t} = & \left\{ (\varepsilon_u^- - 1) a_1(\mathbf{n}) + (\varepsilon_u^+ - 1) \left[\Omega a_2 \left(\frac{\mathbf{n}}{\Omega} \right) + a_3(\mathbf{n}) \right] \right. \\ & \left. (\varepsilon_v^+ - 1) a_4(\mathbf{n}) \right\} P(\mathbf{n}, t) \\ & + \frac{\bar{b}}{a} \sum_{\mathbf{m} \in l(\mathbf{n})} (\varepsilon_v^- - 1) a_3(\mathbf{m}) P(\mathbf{n}, t; \mathbf{m}, t - \tau), \end{aligned} \quad (A1)$$

where reaction propensities together with associated state change vectors are given by

$$a_j(\mathbf{n}) = \begin{cases} rn_u(t), & \mathbf{v}_1 = (1, 0), \\ rn_u(t)^2/K, & \mathbf{v}_2 = (-1, 0), \\ an_v(t)e^{-\alpha n_v(t)/n_u(t)}, & \mathbf{v}_3 = (-1, \bar{b}/a), \\ dn_v(t), & \mathbf{v}_4 = (0, -1). \end{cases}$$

We can expand shift operators

$$\varepsilon_{u,v}^\pm - 1 = \pm \Omega^{-1/2} \frac{\partial}{\partial \xi_{1,2}} + \frac{1}{2} \Omega^{-1} \frac{\partial^2}{\partial \xi_{1,2}^2} \pm \dots$$

and use expansions (11) and (12) for $n_{u,v}(t)$ and $n_{u,v}(t - \tau)$ to obtain

$$\begin{aligned} a_1(\mathbf{n}) &= ru\Omega + ru\xi_1\Omega^{1/2}, \quad a_4(\mathbf{n}) = dv\Omega + d\xi_2\Omega^{1/2}, \\ a_2\left(\frac{\mathbf{n}}{\Omega}\right) &= \frac{r}{K}\left(u^2 + 2u\xi_1\Omega^{-1/2} + \xi_1^2\Omega^{-1}\right), \\ a_3(\mathbf{n}) &= a\left(\Omega v + \Omega^{1/2}\xi_2\right)e^{-\alpha(v+\Omega^{-1/2}\xi_2)/(u+\Omega^{-1/2}\xi_1)} \\ &= ave^{-\alpha v/u}\left\{\Omega + \left[\left(1 - \frac{v}{u}\right)\xi_2 + \left(\frac{v^2}{u^2}\right)\xi_1\right]\Omega^{1/2}\right\} \\ &\quad + \mathcal{O}(\Omega^0). \end{aligned}$$

Substituting these expressions into the DCME (10), rewriting the left-hand side in terms of $\Pi(\xi, t)$, and using the relation (13), we collect terms of the same order of Ω . At the highest order, i.e., $\Omega^{1/2}$, we have

$$\begin{aligned} \dot{u} &= ru(t)\left(1 - \frac{u(t)}{K}\right) - av(t)e^{-\alpha v(t)/u(t)}, \\ \dot{v} &= \bar{b}v(t - \tau)e^{-\alpha v(t-\tau)/u(t-\tau)} - dv(t), \end{aligned}$$

which are nothing else but the original deterministic model (2) describing macroscopic dynamics.

To next order in Ω , i.e., collecting terms $\mathcal{O}(\Omega^0)$, one obtains a delayed Fokker–Planck equation,

$$\begin{aligned} \frac{\partial \Pi(\xi, t)}{\partial t} &= -\frac{\partial}{\partial \xi_2}\left[d\xi_2\Pi(\xi, t)\right] - \frac{\partial}{\partial \xi_1}\left\{\left[r\left(1 - \frac{2u(t)}{K}\right)\xi_1\right.\right. \\ &\quad \left.\left.- ae^{-\alpha v(t)/u(t)}\left[\left(1 - \frac{v(t)}{u(t)}\right)\xi_2 + \left(\frac{v(t)^2}{u(t)^2}\right)\xi_1\right]\right]\Pi(\xi, t)\right\} \\ &\quad - \bar{b}e^{-\alpha v(t-\tau)/u(t-\tau)}\frac{\partial}{\partial \xi_2}\int_{\eta}\left[\left(1 - \frac{v(t-\tau)}{u(t-\tau)}\right)\eta_2\right. \\ &\quad \left.+ \left(\frac{v(t-\tau)^2}{u(t-\tau)^2}\right)\eta_1\right]\Pi(\xi, t; \eta, t - \tau)d\eta \\ &\quad + \frac{1}{2}\left[ru(t)\left(1 + \frac{u(t)}{K}\right) + av(t)e^{-\alpha v(t)/u(t)}\right]\frac{\partial^2 \Pi(\xi, t)}{\partial \xi_1^2} \\ &\quad + \frac{1}{2}\left[\bar{b}v(t - \tau)e^{-\alpha v(t-\tau)/u(t-\tau)} + dv(t)\right]\frac{\partial^2 \Pi(\xi, t)}{\partial \xi_2^2}. \end{aligned} \tag{A2}$$

Since we are interested in the long-time asymptotic limit, where the mean-field trajectory approaches a stable coexistence steady state E^* , we replace in the above equation $u(t) = u(t - \tau) = u^*$ and $v(t) = v(t - \tau) = v^*$ and use relations

$$\begin{aligned} \frac{v^*}{u^*} &= \frac{1}{\alpha}\ln\left(\frac{\bar{b}}{d}\right) \equiv F, \quad \bar{b}v^*e^{-\alpha v^*/u^*} + dv^* = 2dv^*, \\ ru^*\left(1 + \frac{u^*}{K}\right) + av^*e^{-\alpha v^*/u^*} &= 2ru^*, \quad \bar{b}e^{-\alpha v^*/u^*} = 1 \end{aligned}$$

to obtain

$$\begin{aligned} \frac{\partial \Pi(\xi, t)}{\partial t} &= -\frac{\partial}{\partial \xi_2}\left[d\xi_2\Pi(\xi, t)\right] - \frac{\partial}{\partial \xi_1}\left\{\left[r\left(1 - \frac{2u^*}{K}\right)\xi_1\right.\right. \\ &\quad \left.\left.- \frac{ad}{b}\left((1 - F)\xi_2 + F^2\xi_1\right)\right]\Pi(\xi, t)\right\} \\ &\quad - d\frac{\partial}{\partial \xi_2}\int_{\eta}\left[(1 - F)\eta_2 + F^2\eta_1\right]\Pi(\xi, t; \eta, t - \tau)d\eta \\ &\quad + ru^*\frac{\partial^2 \Pi(\xi, t)}{\partial \xi_1^2} + dv^*\frac{\partial^2 \Pi(\xi, t)}{\partial \xi_2^2}, \end{aligned} \tag{A3}$$

which correspond to the system of the delayed Langevin equation (14) describing the dynamics of fluctuations known as the linear noise approximation.

DATA AVAILABILITY

The data that support the findings of this study are available within the article.

REFERENCES

- ¹A. J. Lotka, *Elements of Physical Biology* (Williams and Wilkins, Baltimore, MD, 1925).
- ²V. Volterra, *Nature* **188**, 558 (1926).
- ³G. I. Bell, *Math. Biosci.* **16**, 291 (1973).
- ⁴K. Voskarides, E. Christaki, and G. K. Nikolopoulos, *Front. Immun.* **9**, 2017 (2018).
- ⁵P. A. Samuelson, *Proc. Natl. Acad. Sci. U.S.A.* **68**, 980 (1971).
- ⁶J. R. Carter and C. H. Anderson, *J. Econ. Behav. Org.* **45**, 83 (2001).
- ⁷H. I. Freedman, *Deterministic Mathematical Models in Population Ecology* (Marcel Dekker, Inc., 1980).
- ⁸G. F. Gause, *The Struggle for Existence* (Williams and Wilkins, Baltimore, MD, 1934).
- ⁹A. N. Kolmogorov, *Prob. Cyb.* **25**, 100 (1972).
- ¹⁰M. E. Solomon, *J. Anim. Ecol.* **18**, 1 (1949).
- ¹¹R. Arditi and L. R. Ginzburg, *J. Theor. Biol.* **139**, 311 (1989).
- ¹²R. Arditi and L. R. Ginzburg, *How Species Interact: Altering the Standard View on Trophic Ecology* (Oxford University Press, Oxford, 2012).
- ¹³R. Xu, M. Chaplain, and F. Davidson, *Appl. Math. Comput.* **158**, 729 (2004).
- ¹⁴T. Saha and M. Bandyopadhyay, *Appl. Math. Comput.* **196**, 458 (2008).
- ¹⁵E. Beretta and Y. Kuang, *Nonlinear Anal. TMA* **32**, 381 (1998).
- ¹⁶Y. Kuang, *Fields Inst. Commun.* **21**, 325 (1999).
- ¹⁷M. Haque, *Bull. Math. Biol.* **71**, 430 (2009).
- ¹⁸D. Xiao and S. Ruan, *J. Math. Biol.* **43**, 268 (2001).
- ¹⁹C. Jost, O. Arino, and R. Arditi, *Bull. Math. Biol.* **61**, 19 (1999).
- ²⁰R. Arditi, N. Perrin, and H. Saïah, *Oikos* **60**, 69 (1991).
- ²¹T. Spataro, S. Bacher, L. Bersier, and R. Arditi, *Ecosphere* **3**, 124 (2012).
- ²²C. S. Holling, *Can. Entomol.* **91**, 293 (1959).
- ²³C. S. Holling, *Can. Entomol.* **91**, 385 (1959).
- ²⁴Y. V. Tyutyunov and L. I. Titova, *Biol. Bull. Rev.* **10**, 167 (2020).
- ²⁵J. H. P. Dawes and M. O. Souza, *J. Theor. Biol.* **327**, 11 (2013).
- ²⁶Y. Kuang, *Math. Biosci. Eng.* **4**, 1 (2007).
- ²⁷M. Van Baalen, V. K'rivan, P. C. J. Van Rijn, and M. W. Sabelis, *Am. Nat.* **157**, 512 (2001).
- ²⁸L.-L. Wang, Y.-H. Fan, and W.-T. Li, *Appl. Math. Comput.* **172**, 1103 (2006).
- ²⁹Y.-H. Fan and W.-T. Li, *J. Math. Anal. Appl.* **299**, 357 (2004).
- ³⁰P. J. Pal, P. K. Mandal, and K. K. Lahiri, *Nonlinear Dyn.* **76**, 201 (2014).
- ³¹X. Wang, M. Peng, and X. Lu, *Appl. Math. Comp.* **268**, 496–508 (2015).
- ³²W.-T. Li and S.-L. Wu, *Chaos, Solitons Fractals* **37**, 476 (2008).
- ³³N. Apreutesei and G. Dimitriu, *J. Comp. Appl. Math.* **235**, 366 (2010).
- ³⁴L. N. Guin and P. K. Mandal, *Int. J. Biomath.* **7**, 1450047 (2014).

- ³⁵D. Schenk, L.-F. Bersies, and S. Bacher, *J. Anim. Ecol.* **74**, 86 (2005).
- ³⁶O. Sarnelle and A. E. Wilson, *Ecology* **89**, 1723 (2008).
- ³⁷A. Morozov, *J. Theor. Biol.* **265**, 45 (2010).
- ³⁸P. Kratina, M. Vos, A. Bateman, and B. R. Anholt, *Oecologia* **159**, 425 (2009).
- ³⁹V. S. Ivlev, *Usp. Sovrem. Biol.* **24**, 417 (1947).
- ⁴⁰V. S. Ivlev, *Experimental Ecology of the Feeding of Fishes* (Yale University Press, New Haven, CT, 1961).
- ⁴¹W. E. Ricker, *J. Fisheries Res. Board Can.* **11**, 559 (1954).
- ⁴²J. Holt, M. J. Jeger, J. M. Thresh, and G. W. Otim-Nape, *J. Appl. Ecol.* **34**, 793 (1997).
- ⁴³K. B. Blyuss, F. Al Basir, V. A. Tsygankova, L. O. Biliavska, and G. O. Iutynska *et al.*, *Ric. di Math.* **69**, 437 (2020).
- ⁴⁴F. Al Basir, Y. N. Kyrychko, K. B. Blyuss, and S. Ray, *Bull. Math. Biol.* **83**, 87 (2021).
- ⁴⁵S. A. Gourley and Y. Kuang, *J. Math. Biol.* **49**, 188 (2004).
- ⁴⁶S. Liu and E. Beretta, *SIAM J. Appl. Math.* **66**, 1101 (2006).
- ⁴⁷E. Beretta and Y. Kuang, *SIAM J. Math. Anal.* **33**, 1144 (2002).
- ⁴⁸Y. Kuang, *Delay Differential Equations with Applications in Population Dynamics* (Academic Press, New York, 1993).
- ⁴⁹Z. Zhang, T. Ding, W. Huang, and Z. Dong, *Qualitative Theory of Differential Equations* (American Mathematical Society, Providence, 1991).
- ⁵⁰G. Li, W. Wang, K. Wang, and Z. Jin, *J. Math. Anal. Appl.* **31**, 631 (2007).
- ⁵¹S. Ruan, Y. Tang, and W. Zhang, *J. Math. Biol.* **57**, 223 (2008).
- ⁵²D. Breda, S. Maset, and R. Vermiglio, *Appl. Numer. Math.* **56**, 318 (2006).
- ⁵³J. Mallet-Paret and H. L. Smith, *J. Dyn. Diff. Eqns.* **2**, 367 (1990).
- ⁵⁴J. Mallet-Paret and G. Sell, *J. Diff. Eqns.* **125**, 441 (1996).
- ⁵⁵T. Tian, K. Burrage, P. M. Burrage, and M. Carletti, *J. Comput. Appl. Math.* **205**, 696 (2007).
- ⁵⁶A. Leier and T. T. Marquez-Lago, *Proc. R. Soc. A* **471**, 20150049 (2015).
- ⁵⁷F. Fatehi, Y. N. Kyrychko, and K. B. Blyuss, *Math. Biosci.* **322**, 108327 (2020).
- ⁵⁸X. Cai, *J. Chem. Phys.* **126**, 124108 (2007).
- ⁵⁹N. G. van Kampen, *Stochastic Processes in Physics and Chemistry* (Elsevier, Amsterdam, 1992).
- ⁶⁰T. Galla, *Phys. Rev. E* **80**, 021909 (2009).
- ⁶¹F. Fatehi, Y. N. Kyrychko, and K. B. Blyuss, *Math. Biosci.* **322**, 108323 (2020).
- ⁶²N. E. Phillips, C. S. Manning, T. Pettini, V. Biga, E. Marinopoulou, P. Stanley *et al.*, *Elife* **5**, e16118 (2016).
- ⁶³T. Brett and T. Galla, *Phys. Rev. Lett.* **110**, 250601 (2013).
- ⁶⁴T. Brett and T. Galla, *J. Chem. Phys.* **140**, 124112 (2014).
- ⁶⁵S. Guillouxic, I. L'Heureux, and A. Longtin, *Phys. Rev. E* **59**, 3970 (1999).
- ⁶⁶F. Fatehi, S. N. Kyrychko, A. Ross, Y. N. Kyrychko, and K. B. Blyuss, *Front. Physiol.* **9**, 45 (2018).
- ⁶⁷L. B. Nicholson, K. B. Blyuss, and F. Fatehi, *Cells* **9**, 860 (2020).
- ⁶⁸D. Alonso, A. J. McKane, and M. Pascual, *J. R. Soc. Interface* **4**, 575 (2007).
- ⁶⁹A. J. McKane and T. J. Newman, *Phys. Rev. Lett.* **94**, 218102 (2005).
- ⁷⁰R. Kuske, L. F. Gordillo, and P. Greenwood, *J. Theor. Biol.* **245**, 459 (2007).